Supporting Information

Synthesis and Structural, EPR and Mössbauer Characterizations of a (μ-Alkoxo)(μ-Carboxylato)Diiron(II,III) Model Complex for the Mixed-valent Diiron Active Site of Myo-Inositol Oxygenase

by F. Li, M. Chakrabarti, Y. Dong, K. Kauffmann, E. L. Bominaar, E. Münck, and L. Que, Jr.

Gaussian 03, Revision E.01,
M. J. Frisch, G. W. Trucks, H. B. Schlegel, G. E. Scuseria,
M. A. Robb, J. R. Cheeseman, J. A. Montgomery, Jr., T. Vreven,
K. N. Kudin, J. C. Burant, J. M. Millam, S. S. Iyengar, J. Tomasi,
V. Barone, B. Mennucci, M. Cossi, G. Scalmani, N. Rega,
G. A. Petersson, H. Nakatsuji, M. Hada, M. Ehara, K. Toyota,
R. Fukuda, J. Hasegawa, M. Ishida, T. Nakajima, Y. Honda, O. Kitao,
H. Nakai, M. Klene, X. Li, J. E. Knox, H. P. Hratchian, J. B. Cross,
V. Bakken, C. Adamo, J. Jaramillo, R. Gomperts, R. E. Stratmann,
O. Yazyev, A. J. Austin, R. Cammi, C. Pomelli, J. W. Ochterski,
P. Y. Ayala, K. Morokuma, G. A. Voth, P. Salvador, J. J. Dannenberg,
V. G. Zakrzewski, S. Dapprich, A. D. Daniels, M. C. Strain,
O. Farkas, D. K. Malick, A. D. Rabuck, K. Raghavachari,
J. B. Foresman, J. V. Ortiz, Q. Cui, A. G. Baboul, S. Clifford,
J. Cioslowski, B. B. Stefanov, G. Liu, A. Liashenko, P. Piskorz,
I. Komaromi, R. L. Martin, D. J. Fox, T. Keith, M. A. Al-Laham,
C. Y. Peng, A. Nanayakkara, M. Challacombe, P. M. W. Gill,
B. Johnson, W. Chen, M. W. Wong, C. Gonzalez, and J. A. Pople,
Gaussian, Inc., Wallingford CT, 2004.

S1. Details of parameter extraction from Mössbauer/EPR data of 1

The initial guesses for the ZFS parameters were generated with the scheme in eq 13. Using eq 5, the experimental $\mathcal{A}^{A}_{\xi\xi}$ values (–57.3, –43.0, –46.7) MHz imply the $\mathcal{D}^{e}_{\xi\xi}/J$ values (–0.316, 0.228, 0.088), which yield, for J = 22.5 cm^{-1}, the $\mathcal{D}^{e}_{\xi\xi}$ values (7.10, 5.13, 1.97) cm^{-1}. The EPR g-values for the S = 1/2 ground state are (1.75, 1.88, 1.96) and give, using eq 8, the $g^{B}_{\xi\xi}$ values (2.145, 2.114, 2.033); the corresponding $\Delta g^{B}_{\xi\xi} = g^{B}_{\xi\xi} - 2$ are listed in the first row of Table S1. Using eq 11, the $g^{B}_{\xi\xi}$ values yield the $\mathcal{D}^{B}_{\xi\xi}$ values (–1.90, –0.68, 2.58) cm^{-1}, which represent the main contribution, arising from the S = 2 excited states, to the ZFS of the ferrous site, Fe_B. Assuming that $\mathcal{D}^{B} \approx \mathcal{D}^{B}(S = 2)$, these values yield D_B = 3.88 cm^{-1} and E_B/D_B = –0.16. Finally, eq 12 yields the $\mathcal{D}^{A}_{\xi\xi}$ values (–0.175, 0.898, –0.723) cm^{-1} [D_A = –1.08 cm^{-1} and E_A/D_A = 0.49].

The above example represents one out of 3! = 6 possible ways to associate the principal axes of the g tensor with the collinear axes of the $\mathcal{A}^{A}$ and $\mathcal{D}^{e}$ tensors, which have been adopted as the {x, y, z} frame of reference throughout the SI. The Δg_{ξ}^{B} and ZFS parameters obtained for the six mappings are listed in Table S1.

In each case, the largest Δg_{ξ}^{B} value corresponds to the smallest g_{ξ} value of the coupled system. The D_A and D_B values listed in Table S1 have been associated with the z axis by definition. ZFS parameters which do not fulfill the inequalities $0 \le E_X/D_X \le 1/3$ (X = A, B) can be redefined by taking D_X (X = A, B) along x or y. Table S2 presents the axes for which ZFS parameters appear in standard convention, $0 \le E_X/D_X \le 1/3$. Table S2 shows that D_B is positive when the D_B axis is parallel to the direction for which the g-value is closest to 2, i.e. along the ξ axis (ξ = x, y, or z) for which $g_{\xi} = 1.96$ in Table S1 (this is the axis along which the orbital angular momentum is approximately zero). Alternately, D_B is negative when the D_B axis is perpendicular to the direction ξ for which $g_{\xi} = 1.96$. These properties follow from the $\mathcal{D}^{B}$–Δg^{B} relationship in eq 11.

In the context of a distorted $^5T_2$ crystal-field description for Fe_B, D_B is positive when $E(t_2) > (E(t_3) - E(t_1))/2$, where $\{t_1, t_2, t_3\}$ is the set $\{d_{xy}, d_{xz}, d_{yz}\}$ and the crystal-field splitting energies satisfy the relations $E(t_1) < E(t_2) \le E(t_3)$. D_B is negative when $E(t_2) < (E(t_3) - E(t_1))/2$.

Table S1. g-values of complex **1**, g – 2 values for Fe^{II} site, and zero-field parameters for Fe^{III} (site A) and Fe^{II} (site B)

#	g_x	g_y	g_z	Δg_x^B	Δg_y^B	Δg_z^B	D_B [a,b]	E_B/D_B	D_A [a,b]	E_A/D_A
1	1.75	1.88	1.96	0.145	0.114	0.033	3.88	–0.16	–1.08	0.49
2	1.88	1.75	1.96	0.070	0.238	0.033	4.85	0.70	–1.45	1.40
3	1.75	1.96	1.88	0.145	0.038	0.098	–0.26	8.17	0.47	0.08
4	1.88	1.96	1.75	0.070	0.038	0.204	–6.01	0.10	2.62	–0.20
5	1.96	1.75	1.88	0.023	0.238	0.098	1.31	3.29	–0.12	19.56
6	1.96	1.88	1.75	0.023	0.114	0.204	–5.42	–0.34	2.40	–0.60

[a] Along z axis. [b] In wavenumbers.

Table S2. Zero-field parameters for Fe^{II} (site B) and Fe^{III} (site A) of Table S1 in standard representation[a]

#	D_B [a,b]	Axis D_B	E_B/D_B	D_A [a,b]	Axis D_A	E_A/D_A
1	3.88	z	0.16	1.35	y	0.20
2	–7.49	y	0.10	3.77	y	0.08
3	3.33	y	0.28	0.47	z	0.08
4	–6.01	z	0.10	2.62	z	0.20
5	–7.11	y	0.21	3.63	y	0.31
6	5.44	x	0.03	–3.37	x	0.14

[a] $0 \le E_X/D_X \le 1/3$, X = A, B. [b] In wavenumbers.

Table S3. $(E/D)_B$, D_A, and $(E/D)_B$ obtained using eqs S2a-c and $\mathcal{D}^{e}_{xx}$ = 7.10 cm^{-1}, $\mathcal{D}^{e}_{yy}$ = 5.13 cm^{-1}, $\mathcal{D}^{e}_{zz}$ = 1.97 cm^{-1}, and the value for Q_{cl} with D_B values obtained for the six permutations in Table S1

#	Q [a]	Q_{sc} [b]	Q_{cl} [c]	D_B [d]	E_B/D_B	D_A [d]	E_A/D_A
1	–0.21	0.21	–0.15	3.88	–0.10	–1.08	0.58
2	0.63	0.13	0.59	4.85	0.65	–1.45	1.34
3	15.56	0.31	2.09	–0.26	0.34	0.47	–1.57
4	0.14	0.14	0.15	–6.01	0.11	2.62	–0.20
5	2.87	0.20	2.09	1.31	2.44	–0.12	16.06
6	–0.30	0.30	–0.15	–5.42	–0.19	2.40	–0.49

[a] $Q = (\mathcal{D}^{3/2}_{xx} - \mathcal{D}^{3/2}_{yy})/(3\mathcal{D}^{3/2}_{zz})$ where $\mathcal{D}^{3/2}_{\xi\xi} = -(4/15)\mathcal{D}^{A}_{\xi\xi} - \mathcal{D}^{B}_{\xi\xi}$.

[b] $Q_{sc} = E_{3/2}/D_{3/2}$ in standard convention $0 \le E_{3/2}/D_{3/2} \le 1/3$.

[c] According to eq S1 there are six values for $E_{3/2}/D_{3/2}$ for which this ratio is consistent with the EPR data for S = 3/2. Q_{cl} is among these six values the one closest to the value for Q given in second column.

[d] In wavenumbers.

Table S4. Zero-field parameters for Fe^{II} (site B) and Fe^{III} (site A) of Table S3 in standard representation[a]

# [a]	D_B	Axis D_B [b,c]	E_B/D_B	D_A	Axis D_A [b,c]	E_A/D_A
1	3.88	z	0.10	1.48	y	0.16
2	–7.13	y	0.12	3.64	y	0.07
3	0.26	y	0.33	–1.33	x	0.10
4	–6.01	z	0.11	2.62	z	0.20
5	–5.45	y	0.17	3.01	y	0.31
6	–5.42	z	0.19	–2.92	x	0.21

[a] Numbering of cases defined in Table S1. [b] $0 \le E_X/D_X \le 1/3$, X = A, B. [c] In wavenumbers.

At this juncture, there are six admissible sets of ZFS parameters (Tables S1-2). We now analyze to what extent these sets are consistent with the EPR data for the S = 3/2 excited state. The simulation of the excited S = 3/2 state spectrum gives an estimate for the rhombicity ratio $E_{3/2}/D_{3/2} = 0.15$. It should be noted that this value refers to the standard convention according to which $E_{3/2}/D_{3/2} = (\mathcal{D}^{3/2}_{x'x'} - \mathcal{D}^{3/2}_{y'y'})/(3\mathcal{D}^{3/2}_{z'z'})$ where the {x′, y′, z′} axes are labeled such that $|\mathcal{D}^{3/2}_{x'x'}| \le |\mathcal{D}^{3/2}_{y'y'}| \le |\mathcal{D}^{3/2}_{z'z'}|$. This convention implies $0 \le E_{3/2}/D_{3/2} \le 1/3$. In general, depending on the permutation of {x′, y′, z′} relative to {x, y, z}, E/D defined as $(\mathcal{D}^{3/2}_{xx} - \mathcal{D}^{3/2}_{yy})/(3\mathcal{D}^{3/2}_{zz})$ (N.B. no primes) has one of the following values:

$$\pm E/D,\ \pm\frac{1-E/D}{1+3E/D},\ \pm\frac{1+E/D}{1-3E/D}. \qquad \text{(S1)}$$

Thus, for $E_{3/2}/D_{3/2} = 0.15$, we have the allowed values ±0.15, ±0.5862, and ±2.0909. To test the consistency of the ZFS parameters in Tables S1-2 with the S = 3/2 EPR, we have evaluated $\mathcal{D}^{3/2}_{\xi\xi} = -(4/15)\mathcal{D}^{A}_{\xi\xi} - \mathcal{D}^{B}_{\xi\xi}$ using $\mathcal{D}^{A}_{\xi\xi}$ and $\mathcal{D}^{B}_{\xi\xi}$ values for each of the six cases of Table S1. Subsequently, we have calculated the values for $Q = E/D = (\mathcal{D}^{3/2}_{xx} - \mathcal{D}^{3/2}_{yy})/(3\mathcal{D}^{3/2}_{zz})$ and listed them in 2nd column of Table S3 (again, {x, y, z} is the frame of the $\mathcal{A}^{A}$ and $\mathcal{D}^{e}$ tensors); the 3rd column gives the corresponding rhombicity ratio in standard convention (Q_{sc}). The 4th column lists among the six allowed $E_{3/2}/D_{3/2}$ values the one that is closest (Q_{cl}) closest to the Q value in the 2nd column. The values for $Q_{cl} = Q = (\mathcal{D}^{3/2}_{xx} - \mathcal{D}^{3/2}_{yy})/(3\mathcal{D}^{3/2}_{zz})$ and $\mathcal{D}^{e}_{\xi\xi}$ (ξ = x, y) impose three linear conditions on D_A, E_A, D_B, and E_B. Using these, the quantities D_A, E_A, and E_B can be expressed in terms of D_B, $E_{3/2}/D_{3/2}$, $\mathcal{D}^{e}_{xx}$, and $\mathcal{D}^{e}_{yy}$:

$$D_A = \frac{1}{8}\left(D_e - 3D_B\right) \tag{S2a}$$

$$E_A = \frac{1}{72}\left(10E_e - Q\left(D_e + 27D_B\right)\right) \tag{S2b}$$

$$E_B = \frac{1}{27}\left(-E_e + Q\left(D_e + 27D_B\right)\right), \tag{S2c}$$

where we have introduced the quantities D_e, and E_e, which are defined as $D_e = -\frac{3}{2}\left(\mathcal{D}^{e}_{xx} + \mathcal{D}^{e}_{yy}\right)$ and $E_e = \frac{1}{2}\left(\mathcal{D}^{e}_{xx} - \mathcal{D}^{e}_{yy}\right)$. Since S = 3/2 EPR gives no information about the labeling of the axes for which $E_{3/2}/D_{3/2} = 0.15$, the value of Q to be adopted in eqs 2a-c can be any of the allowed values listed below eq S1. Obviously, the highest degree of consistency is attained by taking in eqs 2Sa-c for Q the allowed Q value closest to the value in the 2nd column, i.e. Q_{cl} (4th column). For example, substitution of $D_B = 3.88$ cm^{-1}, $Q = -0.15$, $\mathcal{D}^{e}_{xx} = -7.10$ cm^{-1}, and $\mathcal{D}^{e}_{yy} = 5.13$ cm^{-1} into eqs S2a-c gives $D_A = -1.08$ cm^{-1}, $E_A/D_A = 0.58$, and $E_B/D_B = -0.10$, values that have been listed in the 1st row of Table S3.

In an analogous manner, we have evaluated the values of D_A, E_A/D_A, and E_B/D_B for the other five D_B entries in Table S1 (see Table S3). Table S4 lists the ZFS parameters of Table S3 in standard convention. A comparison of Tables S4 and S2 shows that the best agreement between the two tables is found for case 4. Slightly less perfect agreements are found for the cases 2, 5, and 1 and the least satisfactory agreements for the cases 6 and 3. The cases with satisfactory agreement {4, 2, 5, 1} contain two subsets. The members of the first subset {4, 2, 5} have a large negative value for D_B (Table S4) and a positive D_A of about half the magnitude of D_B along the same axis (Table S4). The second subset {1} has a positive value for D_B and a positive value for D_A along an axis perpendicular to the axis for D_B. The magnitudes of D_B and D_A are about half those for these parameters in the first subset. The D_A value for the second subset, {1}, is more in line with the value expected for a high-spin ferric site with N/O coordination than the D_A values for the second subset. However, we think that the first subset, {4, 2, 5}, cannot be ruled out on this account. Thus, we have performed simulations of the Mössbauer spectra

for the two subsets. These simulations revealed a clear preference for the second subset, case 1.

Using the ZFS parameters as adjustable variables and the values for case 1 of Table S1 as initial guess, we have performed a numerical fit of the spectra with eq 1. The fit yielded the values D_B = 2.5 cm^{-1}, E_B/D_B = –0.11, D_A = –0.27 cm^{-1}, and E_A/D_A = 2.25, implying that $\mathcal{D}^{B}_{\xi\xi}$(fit) = (–1.11, –0.56, 1.67) cm^{-1} and $\mathcal{D}^{A}_{\xi\xi}$(fit) = (–0.52, 0.70, –0.18) cm^{-1} from which follows that $\mathcal{D}^{e}_{\xi\xi}$(fit) = (–7.47, 3.90, 3.57) cm^{-1} using eq 12. $\mathcal{D}^{e}_{\xi\xi}$(fit) differs moderately from $\mathcal{D}^{e}_{\xi\xi}$ = (–7.10, 5.13, 1.97) cm^{-1} deduced from $\mathcal{A}^{A}$, using eq 5 and J = 22.5 cm^{-1}. $\mathcal{D}^{B}_{zz}$(fit) is smaller than the value for $\mathcal{D}^{B}_{zz}$(S = 2) = 2.58 cm^{-1} [$D_B(S_B = 2)$ = 3.88 cm^{-1}] obtained for case 1. Differences in E_B/D_B as obtained, on the one hand, from eq 11 and, on the other hand, from eqs S2a-c or the Mössbauer fit may arise when the spin–orbit coupling of the S_B = 2 ground state with S_B = 1 excited states gives non-vanishing contributions to the ZFS (see below). In section S3 it is shown that the S_B = 1 contribution to $\mathcal{D}^{B}$ is approximately axial and negative along z. Adding $\mathcal{D}^{B}_{\xi\xi}(S_B = 1)$ = (0.46, 0.46, –0.92) cm^{-1} [$D_B(S_B = 1)$ = –1.38 cm^{-1}] to $\mathcal{D}^{B}_{\xi\xi}(S_B = 2)$ = (–1.90, –0.68, 2.58) cm^{-1} yields $\mathcal{D}^{B}_{\xi\xi}$(total) = (–1.44, –0.22, 1.67) cm^{-1}, reproducing D_B(fit) = 2.5 cm^{-1} and providing a negative, albeit more rhombic, value E_B/D_B = –0.24.

In section 3.4.1 we noticed that the approximate relationship between $g^{B}_{\xi\xi}$ and $g_{\xi\xi}$ given in eq 8 is rather imprecise in the present case. An accurate assessment of this relationship required a more rigorous analysis on the basis of the fundamental Hamiltonian in eq 1. Thus, using eq 1, $g^{B}_{\xi\xi}$ had to be taken as (2.14, 2.08, 2.00) to reproduce the values $g_{\xi\xi}$ = (1.75, 1.88, 1.96) observed for the S = 1/2 ground state (compared with $g^{B}_{\xi\xi}$ = (2.145, 2.114, 2.033) from eq 8). By substituting the $g^{B}_{\xi\xi}$ values obtained from eq 1 into eq 11, we got the improved estimate $\mathcal{D}^{B}_{\xi\xi}(S_B = 2)$ = (–2.67, –0.26, 2.93) cm^{-1} [D_B = 4.40 cm^{-1} and E_B/D_B = –0.27]. The gap between $\mathcal{D}^{B}_{\xi\xi}(S_B = 2)$ = 2.93 cm^{-1} and $\mathcal{D}^{B}_{zz}$(fit) = 1.67 cm^{-1} [D_B = 2.5 cm^{-1}] can be bridged by assuming a matching S_B = 1 contribution, $\mathcal{D}^{B}_{\xi\xi}(S_B = 1)$ = (0.63, 0.63, –1.26) cm^{-1} [$D_B(S_B = 1)$ = –1.90 cm^{-1}], yielding $\mathcal{D}^{B}_{\xi\xi}$(total) = $\mathcal{D}^{B}_{\xi\xi}(S_B = 2)$ + $\mathcal{D}^{B}_{\xi\xi}(S_B = 1)$ = (–2.03, 0.37, 1.67) [E_B/D_B (total) = –0.48]. The value $D_B(S_B = 1)$ = –1.90 cm^{-1} has the predicted sign but is a wavenumber smaller in magnitude than the value $D_B(S_B = 1)$ = –2.9 cm^{-1} obtained from the theoretical analysis given in section S3. The value E_B/D_B (total) = –0.48 is larger than obtained from the simulation.

S2. Estimates of crystal-field splittings from g^B values

The electronic configuration of Fe_B, gleaned from the DFT solution for complex **1**, is approximately $(d_{xy})^2(d_{xz})^1(d_{yz})^1(d_{z^2})^1(d_{x^2-y^2})^1$. The non-vanishing values $\Delta g_x^B = g_x^B - 2$ = 0.14 and $\Delta g_y^B = g_y^B - 2$ = 0.08 are given by the expressions

$$\Delta g_x^B = -\frac{2\lambda}{\Delta_{xy\rightarrow xz}} \tag{S3a}$$

$$\Delta g_y^B = -\frac{2\lambda}{\Lambda_{xy\rightarrow yz}}, \tag{S3b}$$

where $\lambda = -\zeta/4$ is the effective spin–orbit coupling constant for high-spin ferrous site Fe_B and $\Delta_{d\rightarrow d'}$ the excitation energy for the S = 2 retaining $d\rightarrow d'$ transitions, and imply $\Delta_{xy\rightarrow xz}$ = 1143 cm^{-1} and $\Delta_{xy\rightarrow yz}$ = 2000 cm^{-1}, assuming λ = –80 cm^{-1}. The TD-DFT calculations for **1** place excited state orbitals of Fe_B about 1000 cm^{-1} higher in energy at 2184 cm^{-1} (~ d_{xz}) and 3031 cm^{-1} (~ d_{yz}), which is an acceptable discrepancy given the accuracy of these calculations.

S3. S_B = 1 contributions to ZFS of S_B = 2 ground state of site Fe_B

Assuming that the d_{xz} and d_{yz} orbitals are degenerate, the S_B = 1 contribution to the ZFS of the S_B = 2 ground state is axial along z and given by

$$D_B^{S_B=1} = -\zeta^2\left[\frac{\gamma_{x^2-y^2}\gamma_{xz,yz}}{12\Delta_{x^2-y^2\rightarrow\{xz,yz\}}} + \frac{\gamma_{z^2}\gamma_{xz,yz}}{4\Delta_{z^2\rightarrow\{xz,yz\}}} + \frac{\gamma_{xz,yz}\gamma_{x^2-y^2}}{12\Delta_{\{xz,yz\}\rightarrow x^2-y^2}} + \frac{\gamma_{xz,yz}\gamma_{3z^2-r^2}}{4\Delta_{\{xz,yz\}\rightarrow 3z^2-r^2}} - \frac{\gamma_{xz}\gamma_{yz}}{6\Delta_{xz\leftrightarrow yz}}\right] \tag{S4}$$

The theoretical expressions for the excitation energies in terms of Racah parameters B and C and crystal-field splitting $10D_q$ are given in Table S5. The values of the excitation energies listed in the table were obtained using estimates for B, C, and 10Dq from DFT calculations for a system in which Fe_A has been replaced by a diamagnetic Ga^{III} ion. More specifically, 10Dq was estimated to be about 12000 cm^{-1} from TD-DFT calculations for the S_B = 2 state. By combining the 10Dq value, the free-atom ratio C/B ≈ 4.5, and the difference of the SCF energies for the lowest-lying S_B = 1 excited state and the S_B = 2 ground state (both calculated at the optimized structure for S_B = 2) of 9000 cm^{-1} (see first line of Table S5), we obtained B ≈ 700 cm^{-1}. Since the crystal-field splitting between the $\{d_{xz}, d_{yz}\}$ orbital energies is small compared to the overall S_B = 2 to S_B = 1 splitting, $D_B^{S_B=1}$ is approximately axial.

Table S5. Contributions to the ZFS of $S_B = 2$ ground state of Fe_B arising from spin–orbit coupling with $S_B = 1$ excited states

Transition	$\Delta_{d\to d'}$ [a]	$\Delta_{d\to d'}$ (cm^{-1})	$\gamma_d\gamma_{d'}$ [b]	$\Delta D_B^{S_B=1}$ [c,d]
$x^2-y^2 \to \{xz, yz\}$ [e]	7B+5C−10D_q	9000	0.82	−0.78
$z^2 \to \{xz, yz\}$ [e]	11B+5C−10D_q	12000	0.87	−1.86
$\{xz, yz\} \to x^2-y^2$ [e]	22B+5C+10D_q	43000	0.82	−0.16
$\{xz, yz\} \to 3z^2-r^2$ [e]	6B+5C+10D_q	32000	0.87	−0.70
$xz \leftrightarrow yz$ [e]	13B+5C	25000	0.93	+0.63

[a] B = 700 cm^{-1}, C = 3200 cm^{-1}, 10Dq = 12000 cm^{-1}.

[b] Covalency factors estimated from Mulliken populations: γ_{xz} = 0.96, γ_{yz} = 0.96, $\gamma_{x^2-y^2}$ = 0.85, $\gamma_{3z^2-r^2}$ = 0.90.

[c] Using ζ = 320 cm^{-1}.

[d] Sum gives the total $D_B^{S=1}$ = −2.9 cm^{-1}.

[e] Combined contribution of two degenerate transitions.

Table S6. Coordinates of b3lyp/6-311g optimized structure for ferromagnetic state of **1**

Fe	-2.14549505	0.16136435	0.00054995
Fe	1.45615947	-0.66824859	-0.22467545
O	-0.46280831	-0.12511038	-1.01327261
O	-1.38746585	-0.27244580	1.68837572
O	0.80141593	-0.81726399	1.68880510
N	-2.92992817	0.56014102	-2.20813760
N	-3.20402832	-1.57322937	-0.51818950
N	-4.73094319	-2.67474532	-1.73676641
N	-2.11810536	2.23929840	-0.17392330
N	-2.64036240	4.17655512	-1.17131096
N	1.99218921	-0.26580873	-2.48348287
N	3.40978635	-1.47321724	-0.41854167
N	5.14026872	-2.09939651	-1.70368801
N	2.26468008	1.28758184	-0.13937436
N	3.42516925	2.96010856	-1.08826615
N	-4.12572537	0.63667064	1.06728227
N	0.81569855	-2.83779477	-0.46574990
C	-0.43768999	0.32577329	-2.38739242
H	-0.25491962	1.40729421	-2.39815436
C	-1.79559921	0.01722725	-3.02930826
H	-1.85371052	0.40026897	-4.05367819
H	-1.91116972	-1.06479081	-3.06263714
C	0.67336792	-0.40015855	-3.16291462
H	0.43020104	-1.46112772	-3.18742948
H	0.71533042	-0.03406355	-4.19662151
C	-4.16577801	-0.26772338	-2.38938071
H	-4.34668842	-0.48390667	-3.44646991
H	-5.01789276	0.30701576	-2.02206483
C	-4.02525162	-1.51890678	-1.57827581
C	-3.38705539	-2.84047308	0.06884072
C	-4.34312193	-3.54297470	-0.69753518
C	-4.76012488	-4.83406477	-0.36292688
H	-5.49297648	-5.37373458	-0.94457749
C	-4.19376943	-5.40120756	0.77601853
H	-4.49690771	-6.39309856	1.07817000
C	-3.24539879	-4.70154561	1.55482275
H	-2.85294507	-5.16928479	2.44664297
C	-2.82792039	-3.41685986	1.21449141
H	-2.12402203	-2.87272411	1.82436542
C	-5.71778007	-2.99791636	-2.79656393
H	-6.15884666	-2.06290360	-3.13967377
H	-6.51889611	-3.56193201	-2.32104472
C	-5.10947845	-3.78348692	-3.96079932
H	-5.88468416	-4.01524493	-4.69123620

H	-4.67669873	-4.72485842	-3.62387141
H	-4.33158026	-3.21078135	-4.46824921
C	-3.16051541	2.02410988	-2.42802836
H	-4.23181751	2.20830770	-2.53245092
H	-2.70359154	2.34080156	-3.36963691
C	-2.62307222	2.81607982	-1.27385465
C	-1.78407882	3.28248531	0.71418145
C	-2.10517333	4.50681491	0.09018580
C	-1.90690756	5.73639076	0.72266063
H	-2.15313754	6.67622802	0.25062381
C	-1.37662970	5.69995124	2.01025226
H	-1.21020511	6.62733728	2.53864035
C	-1.05732521	4.47937874	2.64275946
H	-0.65121447	4.49852790	3.64347697
C	-1.25624608	3.25641188	2.00829755
H	-1.01849705	2.32363667	2.49546651
C	-3.11420042	5.15230994	-2.18053825
H	-3.85610980	4.65555654	-2.80512325
H	-3.63937886	5.93884673	-1.64033690
C	-1.98243259	5.73596128	-3.03056210
H	-2.38858733	6.46396100	-3.73295000
H	-1.47424388	4.96153025	-3.60761191
H	-1.24302340	6.24423952	-2.41245190
C	2.96363405	-1.34775237	-2.84573763
H	3.53706667	-1.08833913	-3.74037855
H	2.38870915	-2.24376717	-3.08489494
C	3.85498461	-1.62692135	-1.67223109
C	4.45652001	-1.86471372	0.43243955
C	5.54900079	-2.26765435	-0.36616335
C	6.75182433	-2.70791373	0.19388430
H	7.59201878	-3.01924128	-0.40928456
C	6.82527725	-2.72940709	1.58404682
H	7.73674045	-3.06214852	2.05884886
C	5.73771995	-2.32425302	2.38956253
H	5.84427603	-2.35407828	3.46431430
C	4.54281438	-1.88597105	1.82845387
H	3.71143142	-1.56589073	2.43922204
C	5.96236072	-2.43621493	-2.88784391
H	6.98862808	-2.16134314	-2.64877376
H	5.65043571	-1.79216385	-3.70952227
C	5.87035780	-3.91251285	-3.28406039
H	6.52444845	-4.10706155	-4.13425118
H	4.85472959	-4.18745429	-3.57308938
H	6.18153636	-4.56268009	-2.46703793
C	2.59276823	1.10245162	-2.61182792
H	1.97817010	1.70486279	-3.28709252

H	3.57122330	1.02183776	-3.09223497
C	2.74176028	1.78717903	-1.28345160
C	2.66535508	2.17383913	0.88027407
C	3.38731131	3.23391797	0.29161879
C	3.93911008	4.26990693	1.04957098
H	4.49592092	5.08074585	0.60282958
C	3.75221086	4.20690024	2.42825291
H	4.17060012	4.98217351	3.05368197
C	3.04163096	3.14475920	3.02789433
H	2.93666903	3.12661032	4.10333043
C	2.49059339	2.11753421	2.26714201
H	1.96734121	1.29323894	2.72634036
C	4.08054410	3.81000351	-2.10459983
H	4.36634577	3.17572174	-2.94334950
H	5.00655415	4.17865596	-1.66519611
C	3.20151179	4.97233671	-2.57547874
H	3.74665153	5.57840749	-3.29942982
H	2.91893701	5.61642739	-1.74318149
H	2.28962398	4.61324154	-3.05606597
C	-0.29614545	-0.66904060	2.32635581
C	-0.38581829	-0.92849665	3.76852836
C	0.74017066	-1.41025670	4.46384369
H	1.65737498	-1.58944376	3.92281911
C	0.66329692	-1.65781514	5.83176311
H	1.52765464	-2.02868464	6.36364011
C	-0.53403978	-1.42719498	6.51956102
H	-0.59091537	-1.61870174	7.58177571
C	-1.65766703	-0.94991903	5.83489113
H	-2.57911764	-0.77374556	6.37138795
C	-1.58788080	-0.70201649	4.46602385
H	-2.44848519	-0.33363085	3.92773957
C	-5.00813700	0.86539703	1.78864852
C	-6.10439395	1.15138850	2.69824535
H	-6.40629661	0.24917858	3.23108296
H	-6.96924442	1.53225344	2.15398684
H	-5.80580416	1.90181992	3.43101972
C	0.67485799	-3.98300925	-0.32048488
C	0.51078946	-5.41233489	-0.11491184
H	1.21731456	-5.77077712	0.63466914
H	0.68704252	-5.96261128	-1.03952912
H	-0.49951859	-5.63286305	0.23070467

Table S7. Coordinates of b3lyp/6-311g optimized structure for broken symmetry state of complex **1**

Fe	2.137106	0.368137	0.126718
O	0.397637	0.368681	-0.780335
O	1.437850	0.449692	1.884715
O	-0.815679	0.418095	2.051178
N	2.866754	0.380218	-2.143150
N	2.752190	2.332096	-0.239016
N	3.918111	3.875454	-1.372124
N	2.575059	-1.625201	-0.277035
N	3.454407	-3.286876	-1.495005
N	-2.128086	0.106158	-2.157299
N	-3.665621	0.709604	0.084865
N	-5.558314	1.067171	-1.069508
N	-1.897918	-1.732049	-0.023424
N	-2.739738	-3.495508	-1.132571
C	0.375716	0.067113	-2.198688
C	1.592434	0.728494	-2.856628
C	-0.909186	0.613790	-2.841316
C	3.872372	1.483242	-2.275534
C	3.501965	2.578729	-1.324729
C	2.677224	3.539289	0.483713
C	3.404345	4.518460	-0.228545
C	3.537436	5.829583	0.236255
C	2.923451	6.130899	1.449339
C	2.203517	5.155208	2.173697
C	2.068370	3.850608	1.704344
C	4.740553	4.527839	-2.420977
C	3.900179	5.270565	-3.462757
C	3.404798	-0.962416	-2.531097
C	3.127568	-1.964017	-1.451294
C	2.540127	-2.796790	0.508643
C	3.086987	-3.849490	-0.255770
C	3.209117	-5.146909	0.246909
C	2.767468	-5.357353	1.551009
C	2.224233	-4.308979	2.323770
C	2.104086	-3.017494	1.818386
C	4.071658	-4.027528	-2.620383
C	3.048330	-4.759152	-3.492892
C	-3.331400	0.976401	-2.349649
C	-4.198496	0.903364	-1.127727
C	-4.728351	0.747728	1.002420
C	-5.923981	0.979106	0.287562
C	-7.164049	1.063996	0.927378
C	-7.167814	0.906780	2.310716

C	-5.976317	0.672200	3.032700
C	-4.744473	0.588092	2.392284
C	-6.495172	1.343105	-2.181570
C	-6.761032	2.836957	-2.388029
C	-2.418567	-1.336866	-2.437741
C	-2.331507	-2.187125	-1.202345
C	-2.035933	-2.796790	0.888481
C	-2.556164	-3.912788	0.198762
C	-2.827072	-5.123953	0.840832
C	-2.567689	-5.181104	2.208074
C	-2.057412	-4.066991	2.908985
C	-1.785117	-2.864469	2.263070
C	-3.270029	-4.341768	-2.221782
C	-2.199947	-5.215889	-2.882728
C	0.321213	0.483911	2.614172
C	0.460367	0.597751	4.070689
C	-0.692524	0.660810	4.877507
C	-0.571800	0.769531	6.259913
C	0.696803	0.817526	6.850717
C	1.846946	0.757778	6.055036
C	1.733120	0.648409	4.671285
H	0.421322	-1.021542	-2.320218
H	1.668917	0.464989	-3.916606
H	1.466414	1.807308	-2.782953
H	-0.905590	1.696959	-2.732422
H	-0.920497	0.377679	-3.913473
H	3.935335	1.840711	-3.307550
H	4.852492	1.086110	-2.005951
H	4.094912	6.580619	-0.303865
H	3.011179	7.129653	1.851581
H	1.766331	5.425772	3.124373
H	1.540859	3.100224	2.271703
H	5.358951	3.761643	-2.886709
H	5.421361	5.207777	-1.910995
H	4.556692	5.748246	-4.190060
H	3.290483	6.047598	-3.002905
H	3.239441	4.591060	-4.003341
H	4.482093	-0.886623	-2.693135
H	2.974372	-1.280969	-3.484457
H	3.627789	-5.955379	-0.334321
H	2.845981	-6.344755	1.981980
H	1.896858	-4.516767	3.331909
H	1.695961	-2.216840	2.414888
H	4.652935	-3.318932	-3.209928
H	4.783615	-4.727995	-2.186241
H	3.563923	-5.304171	-4.283721

H	2.352780	-4.063168	-3.964961
H	2.472432	-5.478705	-2.911766
H	-3.882193	0.704955	-3.255235
H	-2.982278	2.001275	-2.485568
H	-8.082867	1.242615	0.388330
H	-8.104649	0.964273	2.845514
H	-6.030385	0.553643	4.105265
H	-3.831547	0.402441	2.939019
H	-7.418950	0.811966	-1.956648
H	-6.088095	0.891390	-3.085794
H	-7.484804	2.975063	-3.191570
H	-5.850329	3.371965	-2.661993
H	-7.169225	3.295154	-1.487729
H	-1.730005	-1.702610	-3.205355
H	-3.418189	-1.424076	-2.871056
H	-3.229401	-5.979272	0.317720
H	-2.772321	-6.095262	2.746360
H	-1.887893	-4.151207	3.973023
H	-1.415617	-2.004339	2.799718
H	-3.746205	-3.691551	-2.955392
H	-4.060738	-4.956597	-1.793828
H	-2.653270	-5.830518	-3.660753
H	-1.731398	-5.882152	-2.158818
H	-1.419456	-4.608960	-3.345418
H	-1.665432	0.627802	4.409898
H	-1.456609	0.817522	6.878198
H	0.788096	0.901300	7.924452
H	2.822857	0.796283	6.517635
H	2.612677	0.601883	4.046603
Fe	-1.563748	0.359178	0.116034
N	4.266314	0.254352	1.020299
C	5.222938	0.163993	1.674834
C	6.412496	0.049434	2.501284
H	6.564406	0.958746	3.083606
H	7.297439	-0.113729	1.885261
H	6.318295	-0.790360	3.190608
N	-1.431588	2.619871	0.169631
C	-1.576247	3.738629	0.452999
C	-1.768929	5.128483	0.832312
H	-2.482670	5.201408	1.653765
H	-2.152445	5.712392	-0.004787
H	-0.825441	5.568901	1.155800

Table S8. Selected parameters in b3lyp/6-311g optimized structure for ferromagnetic state (F.S.) and broken symmetry state (B.S.) of **1** (distances in Å and angles in degrees)

	F.S.	B.S.
Fe···Fe	3.703	3.701
Fe-O-Fe	127.4	127.9
Fe2-O3	2.028	2.076
Fe2-O1	2.145	2.157
Fe2-N6	2.356	2.356
Fe2-N12	2.275	2.265
Fe2-N9	2.118	2.122
Fe2-N7	2.121	2.131
Fe1-O2	1.900	1.894
Fe1-O1	1.985	1.962
Fe1-N1	2.376	2.384
Fe1-N11	2.300	2.312
Fe1-N4	2.085	2.080
Fe1-N2	2.097	2.090

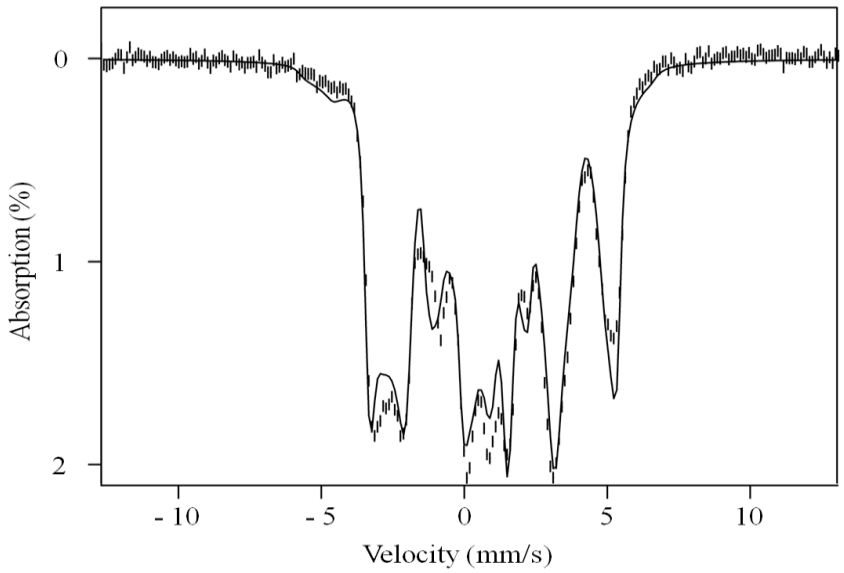

Figure S1. Mössbauer spectra of solid **1** recorded at 4.2 K in a parallel field of 7.63 T. The solid lines through the data are spectral simulations based on eq 1, using the parameters listed in Table 4.